

論文 / 著書情報  
Article / Book Information

Title	Numerical analysis of gypsum board subjected to bending moment using fiber model
Authors	Sakuraba Fumihiko, Alex Shegay, Sato Yasuaki, SHOJIRO MOTOYUI
Citation	Fifth International Workshop on the Seismic Performance of Non-Structural Elements
Pub. date	2022, 12

# Numerical analysis of gypsum board subjected to bending moment using fiber model

Fumihiko Sakuraba<sup>1</sup>, Alex Shegay<sup>2</sup>, Yasuaki Sato<sup>3</sup> and Shojiro Motoyui<sup>4</sup>

<sup>1</sup> Corporate Officer, Someno Construction Materials Co., Ltd.  
648 Shishiko-cho, Ushiku-shi, Ibaraki 300-1231, Japan  
[sakuraba@someno.co.jp](mailto:sakuraba@someno.co.jp)

<sup>2</sup> Assistant Professor, Tokyo Institute of Technology, Japan  
G5, 4259 Nagatsuta, Midori-ku, Yokohama, Kanagawa 226-8502, Japan  
[shegay.a.aa@m.titech.ac.jp](mailto:shegay.a.aa@m.titech.ac.jp)

<sup>3</sup> Researcher, Research&Development, Takenaka Corporation  
1-5-1 Ohtsuka, Inzai-shi, Chiba 270-1395, Japan  
[satou.yasuaki@takenaka.co.jp](mailto:satou.yasuaki@takenaka.co.jp)

<sup>4</sup> Professor, Tokyo Institute of Technology, Japan  
G3, 4259 Nagatsuta, Midori-ku, Yokohama, Kanagawa 226-8502, Japan  
[motoyui.s.aa@m.titech.ac.jp](mailto:motoyui.s.aa@m.titech.ac.jp)

**Abstract.** The in-plane force and bending moment simultaneously occur on gypsum boards which are used in the drywall partition walls, due to the composite beam effect. The mechanical performance of gypsum boards has been tested for pure compression/tension, but the behavior when subjected to simultaneous in-plane force and out-of-plane bending moment demands is unclear. In this paper, a model is proposed to predict the bending behavior of gypsum boards using the results obtained from pure compressive/tensile tests. The purpose of this study is to establish a method to simulate the behavior of gypsum boards subjected to simultaneously axial and bending moment demands. Particularly, the gypsum board is a composite material consisting of gypsum (core material) and base papers. Similar to calculation of non-linear bending behavior of reinforced concrete members, a fiber modelling approach is adopted to perform numerical analysis of gypsum boards subjected to bending moment. This model can also simulate the post cracking behavior macroscopically. On applying the fiber model to the gypsum board, three stress-strain curves are necessary: two curves of gypsum boards in compression/tension and one curve of the base paper in tension. The "effective" curves of pure gypsum in compression/tension were obtained as the difference between the performance of the composite gypsum board and that of the base paper in isolation. The effective stress-strain curve of gypsum, especially one in tension, was found to be higher than that obtained by testing the pure gypsum in isolation. This difference is attributed to the so-called tension stiffening effect in the gypsum material. Finally, to validate the proposed fiber model we show that the numerical results are in good agreement with experimental data.

**Keywords:** Gypsum board, Base paper, Tension stiffening effect, Numerical analysis.

# 1. INTRODUCTION

Following the April 16, 2016 M7.0 Kumamoto earthquake and the March 16, 2022 M7.3 Fukushima earthquake, several accounts of ceiling and partition wall damage were confirmed in media (Figure 1). Eleven years have passed since the 2011 Tohoku Earthquake, but there are still issues with the earthquake resistance of walls and ceilings due to the lightweight steel base material (LGS). Although the breaking load of the gypsum board that composes the LGS wall/ceiling surface has been confirmed by the bending test of JIS A 6901 [JIS, 2013], the data for defining the stress-strain curve of the gypsum board has not been provided. In addition, while in-plane force and bending moment generally act simultaneously on the gypsum board mounted on the LGS (due to the composite beam effect), most existing experimental data have only considered the characteristics of uniaxial compression or tension of the gypsum board [Y. Sato *et al.*, 2020]. Abdelhalim [1995] has previously examined the basic mechanical properties of gypsum boards by uniform compression/tensile testing and bending testing. The study attempted to use statistical methods to address the inconsistency between the stress-strain relationship obtained from bending tension and from uniform tension; however, only qualitative results were obtained. Therefore, there are still many unclear points about the behavior when in-plane force and bending act on the gypsum board at the same time. In considering the earthquake resistance of LGS walls and ceilings, it is important to develop a mechanical understanding of the above points. The objective of this study is to develop a modelling approach for gypsum boards subjected to bending moment demands, founded on experimental results obtained from uni-axial material testing. The focus will be on interpretation and implementation of material test data with consideration to composite action effects, with less focus on the exact material properties and their expected statistical variation.



(a) Kumamoto earthquake (April 2016)

(b) Fukushima earthquake (March 2022)

Figure 1. Example of earthquake damage of non-structural elements following earthquakes in Japan.

## 2. UNIFORM LOADING TEST

### 2.1 OUTLINE OF TEST

Axial testing was carried out on the gypsum board ( $t = 9.5$  mm) to establish mechanical properties. The gypsum board is a three-layer composite board in which two surfaces of the core gypsum material are covered with base paper. Presently, there is no unified standard in Japan for the characteristics of the gypsum board material components, so properties can differ from maker to maker. For the gypsum board adopted in this study, the unit weight was measured to be  $6.7$  kg/m<sup>2</sup>, and the base paper grammage was measured to be  $173$  g/m<sup>2</sup>. The base paper thicknesses are listed in Table 1. It is generally considered that the base

paper has anisotropy derived from the fiber direction of the paper during the papermaking process by a paper machine ([T. Yokoyama *et al.*, 2007]). Therefore, the uniaxial loading test of the gypsum board was carried out in the longitudinal and transverse direction of the base paper. Considering the length of the gypsum board as the parallel direction of the base paper fibers and the short side as the orthogonal direction of the base paper fibers, three test pieces are sampled as shown in Figure 2. A separate set of test pieces were prepared for each tensile and compressive testing.

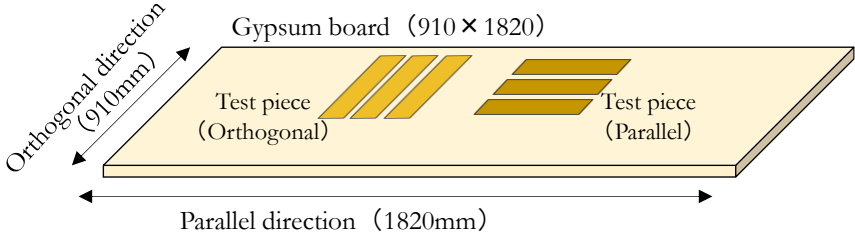


Figure 2. Sampling the test pieces

The tensile test piece of the gypsum board is dogbone-shaped (Figure 3 (a)), and the compression test piece is strip-shaped [Y. Sato *et al.*, 2020]. The base paper test pieces were collected from the gypsum board by separating them with a band saw. The base paper test pieces were taken both from the front (yellow paper) and back (gray paper) of the gypsum board. Figure 3 (b) shows the shape of the tensile test piece of the base paper. All test pieces are shown in Table 1. The width  $B$  and thickness  $t$  of the test piece are average values measured at the center and both ends of the test piece with a caliper. The measured quantities included the load,  $F$ , as measured by the testing machine; the displacement,  $\delta$ , of the chuck that grips the test piece and the strain from the strain gauges attached to the center of the test piece. All gypsum board test pieces had strain gauges on the front and back surfaces. For the test piece of the base paper, the strain gauge was attached only on the outer surface. It is noted that unlike the base paper, the gypsum material does not possess anisotropic properties due to its random crystalline structure.

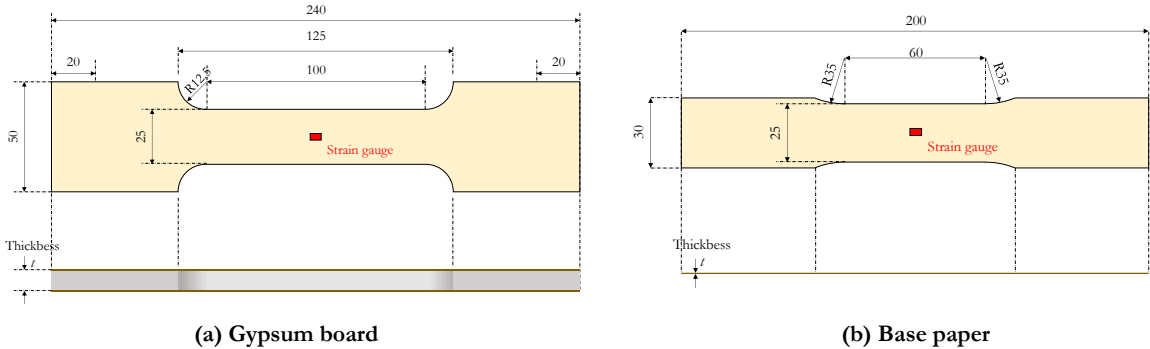


Figure 3. Size of tensile test pieces.

**Table 1. List of the test pieces.**

No.	Name	Material	Load type	Fiber Direction	Average [mm]	
					Width ( $B$ )	Thickness ( $t$ )
1	Gp-T-P-1	Gypsum board (Composite board)	Tensile	Parallel	24.53	9.74
2	Gp-T-P-2				24.49	9.71
3	Gp-T-P-3				24.79	9.70
4	Gp-T-O-1			Orthogonal	24.72	9.70
5	Gp-T-O-2				24.66	9.70
6	Gp-T-O-3				24.51	9.69
7	Gp-C-P-1		Compression	Parallel	49.53	9.71
8	Gp-C-P-2				49.78	9.72
9	Gp-C-P-3				49.74	9.71
10	Gp-C-O-1			Orthogonal	49.85	9.73
11	Gp-C-O-2				49.74	9.67
12	Gp-C-O-3				48.72	9.70
13	Pa-f-T-P-1	Yellow paper (Front)	Tensile	Parallel	25.06	0.24
14	Pa-f-T-P-2				25.11	0.29
15	Pa-f-T-P-3				25.17	0.24
16	Pa-f-T-O-1		Orthogonal	24.66	0.26	
17	Pa-f-T-O-2			25.26	0.24	
18	Pa-f-T-O-3			24.47	0.23	
19	Pa-b-T-P-1	Gray paper (Back)	Tensile	Parallel	25.15	0.23
20	Pa-b-T-P-2				24.77	0.23
21	Pa-b-T-P-3				25.09	0.23
22	Pa-b-T-O-1			Orthogonal	24.99	0.22
23	Pa-b-T-O-2				24.78	0.23
24	Pa-b-T-O-3				24.96	0.23

## 2.2 RESULTS OF UNIFORM LOADING TEST

First, the results of the tensile test of the base paper in the parallel and orthogonal direction are shown in Figure 4 (a) and 5 (a), respectively. Considering the uncertainty of the thickness of the base paper, the vertical axis is expressed as the load  $F$  divided by the width  $B$  of the test piece. The horizontal axis is the longitudinal strain,  $\varepsilon_p$ , measured by the strain gauges. Data is shown up until the test piece breaks. It is clear that the stiffness and strength of the base paper are higher in the parallel direction than in the orthogonal direction due to the material anisotropy. On the other hand, the difference between the base paper properties from the front (yellow paper) and back (gray paper) of the gypsum board are small. This result is also consistent with previous research results [Abdelhalim, 1995]. The average of the stress-strain curves in Figures 4 (a) and 5 (a) are approximated by a cubic function (in the range  $0 \leq \varepsilon_p \leq 7500$ ), represented by the black dotted line. Next, the results of the tensile test of gypsum board and gypsum are shown in Figure 4 (b)~(c), 5 (b)~(c). The horizontal axis is the strain  $\varepsilon$  obtained by dividing the displacement recorded by the test machine,  $\delta$ , (excluding the deformation of the loading jig) by the total length,  $L$ , of the test piece. The “effective” stress-strain curve of the gypsum (Figure 4 (c), 5 (c)) is obtained by subtracting the curves of the two sheets of base paper approximated by a cubic function (black dotted line) from the stress-strain curve of the gypsum board (Figure 4 (b), 5 (b)). The solid black lines in Figure 4 (c) and 5 (c) are the results of the tensile test of the gypsum in isolation, after removal of the base paper. By comparing Figure 4 (b) and 5 (b), it can be recognized that the gypsum board has anisotropy similar to that of the base paper. Comparing the black solid lines in Figure 4 (c) and 5 (c), it can be seen that the difference depending on the fiber direction is small. From this, it is considered that the anisotropy of the gypsum board may be influenced by the anisotropy of the base paper. The “effective” gypsum properties (blue line) in Figure 4 (c) and 5 (c) clearly shows tougher performance in tension compared to when the gypsum is tested in isolation (solid black line). It is considered that the tension stiffening effect [H. Yoshikawa *et al.*, 1986], analogous to that seen in RC members, is the reason the gypsum material is tougher when in the gypsum board configuration than in isolation. The results of the compression test are organized in the same way as in Figures 4 and 5, assuming that compressive properties of the base paper are identical to the tensile properties (Figure 6). It can be confirmed that the influence of the anisotropy of the base paper on the performance of the gypsum board is smaller in compression than in tension. Figure 6 shows a softening response of the gypsum board after the maximum compressive strength is reached.

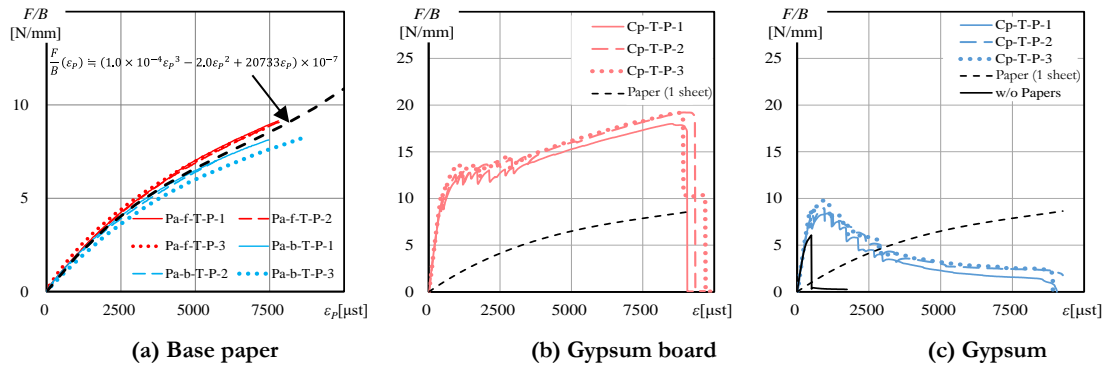


Figure 4. The relationship between  $F/B$  and  $\epsilon$  of each material against the tensile load in the parallel direction.

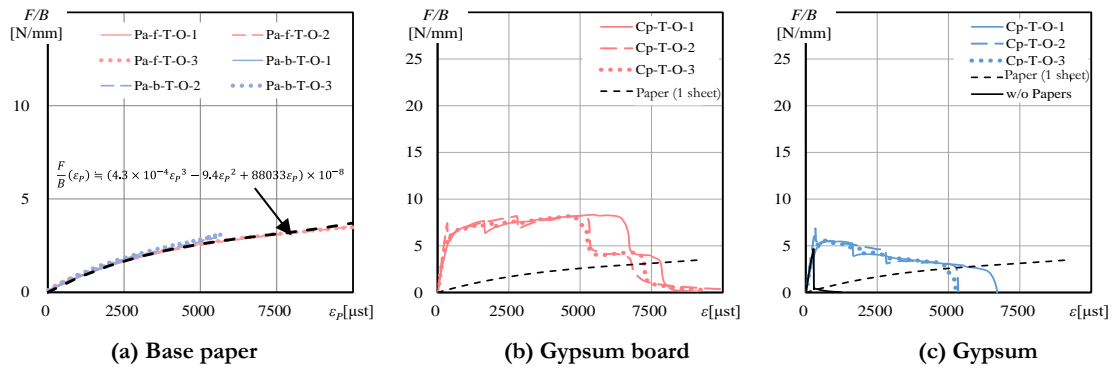


Figure 5. The relationship between  $F/B$  and  $\epsilon$  of each material against the tensile load in the orthogonal direction.

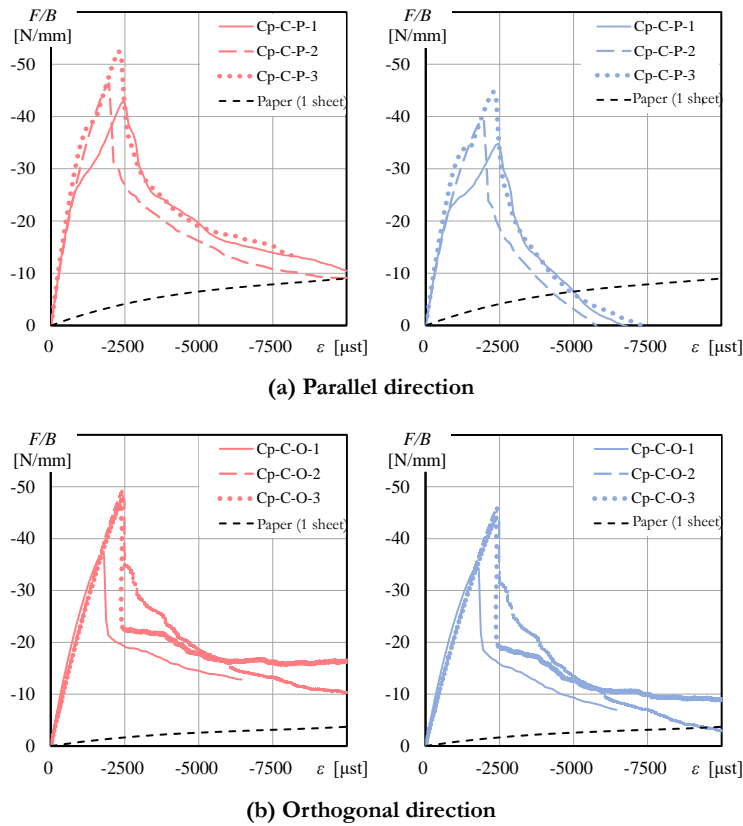


Figure 6. The relationship between  $F/B$  and  $\epsilon$  of each material against the compressive load.

### 3. NUMERICAL ANALYSIS OF GYPSUM BOARD

#### 3.1 OUTLINE OF FIBER MODEL

Figure 7 shows the gypsum board subjected to pure out-of-plane bending. Considering the gypsum as the concrete and the base paper as the reinforcing bar, the gypsum board composite can be analogous to the composition of RC members. In the relationship between the moment and the curvature in the cross section of the RC member, the flexural stiffness gradually decreases due to the progression of cracks. Therefore, the fiber model is often used as a method for evaluating the non-linear flexural behavior of RC members. In this section, the fiber model is also used to perform cross-sectional analysis of the gypsum board.

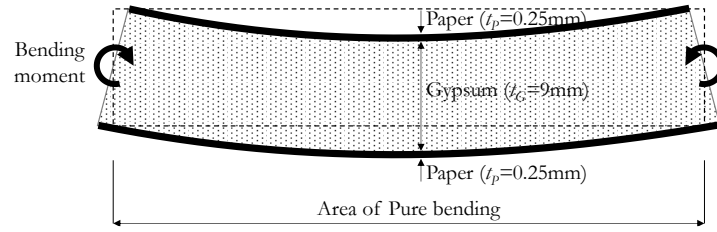


Figure 7. Gypsum board in pure bending.

When the cross section is divided into multi-layered fiber elements as shown in Figure 8, the total bending moment is obtained by the following equation.

$$M = \int_A \sigma y dA = \sum_{i=1}^n \sigma_{G,i} \cdot y_i \cdot A_{G,i} + \sum_{j=1}^m \sigma_{P,j} \cdot y_j \cdot A_{P,j} \quad (1)$$

Here,  $\sigma$ : stress of each fiber element,  $A$ : section area of each fiber element,  $y$ : distance from the centroid of each fiber element to the section centroid,  $n$ : number of divisions of gypsum cross section,  $m$ : number of base papers, lower right subscript  $i, j$ : element number, lower right subscript  $G, P$ : gypsum and base paper. The total axial force on the section is as follow.

$$R_G = \sum_{i=1}^n \sigma_{G,i}(\varepsilon_{G,i}) \cdot A_{G,i} = C_G + T_G \quad (2)$$

$$R_P = \sum_{j=1}^m \sigma_{P,j}(\varepsilon_{P,j}) \cdot A_{P,j} = C_P + T_P \quad (3)$$

Where,  $C$ : total compression force,  $T$ : total tensile force,  $R$ : sum of  $C$  and  $T$ . Then, the force balance equation in the cross section is as follows, and the convergence calculation is performed while changing the neutral axis position  $y_0$  until section force equilibrium ( $N = 0$ ) is reached.

$$N = R_G + R_P \quad (4)$$

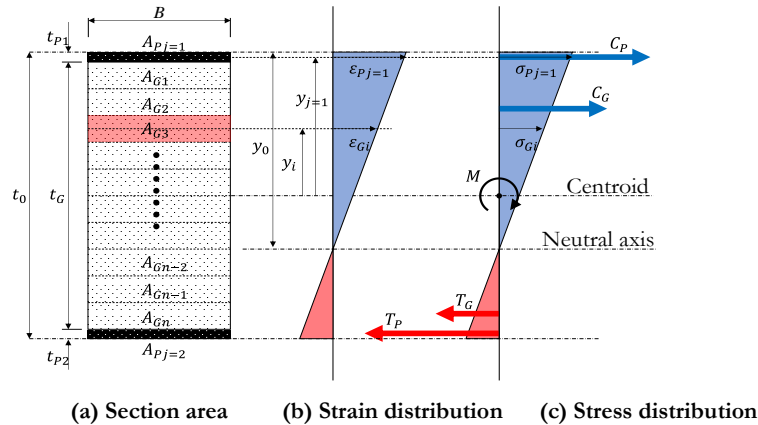


Figure 8. Distribution of strain and stress of gypsum board in pure bending.

### 3.2 MODEL OF MECHANICAL PROPERTY

The material properties of gypsum and base paper used for cross-sectional analysis of gypsum board subject to bending moment are obtained from the results of uniform tensile and compression tests of gypsum board, base paper, and gypsum shown in Figure 9 and 10. The tensile characteristics of the base paper are approximated by a cubic function (thick black line in Figure 9 and 10). The compressive characteristics of the base paper are taken to be equal to the tensile characteristics. The gypsum material model (blue solid line in Figure 9 and 10) is assigned to trace the experimental results. The solid red line shown in Figure 9 and 10 is the sum of gypsum and base paper material model curves, and represents the response of the gypsum board. The cross-section analysis is performed using these material models.

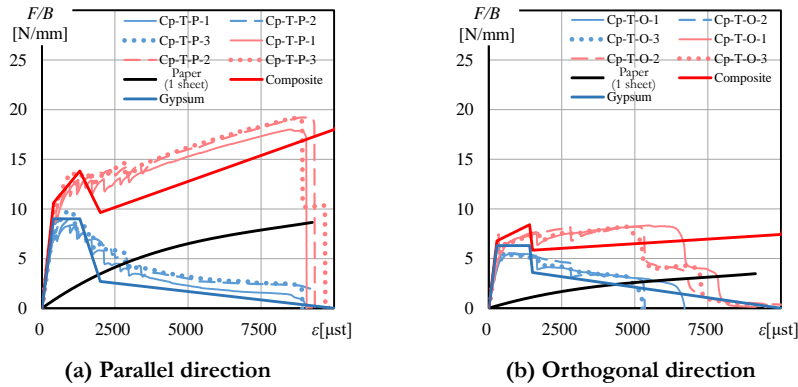


Figure 9. Model of the relationship between  $F/B$  and  $\epsilon$  (Tensile)

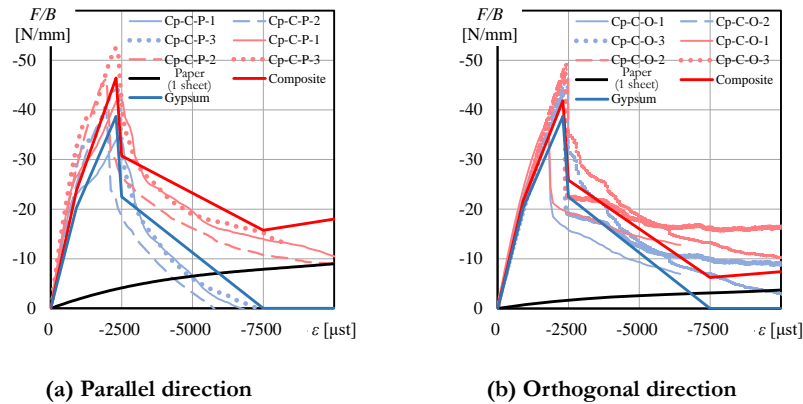


Figure 10. Model of the relationship between  $F/B$  and  $\epsilon$  (Compression)

### 3.3 VALIDITY OF NUMERICAL ANALYSIS

The 4-point bending test of a gypsum board shown in Figure 11 is the target of cross-section analysis. The test piece has strain gauges installed in the center of the pure bending section (front surface:  $\epsilon_f$ , back surface:  $\epsilon_b$ ). The curvature  $\kappa$  is obtained by dividing the strain difference by the thickness  $t$  of the gypsum board. The moment  $M$  is obtained by using the loading force  $P$  and the support distance  $L$ . Two types of gypsum boards with different thicknesses ( $t = 9.5 \text{ mm}$ ,  $12.5 \text{ mm}$ ) were each tested in two fiber direction configurations (parallel/orthogonal). Two test pieces were tested under each of these configurations.

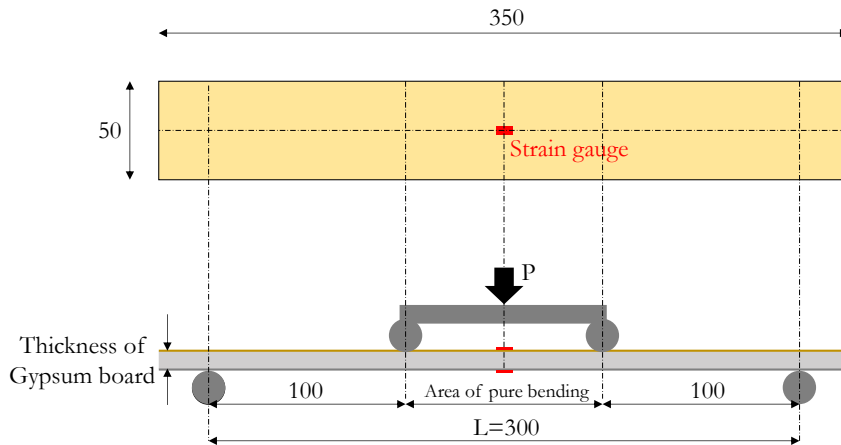


Figure 11. Set up and dimensions of a 4-point bending test of the gypsum board (units: mm).

The moment-curvature ( $M'$ - $\kappa$ ) relationship obtained from cross-sectional analysis of the gypsum board test pieces is compared with the experimental results in Figure 12. Here, the vertical axis of Figure 12 is the moment  $M'$  [Nmm/mm] per unit width of the gypsum board. The material properties used for the cross-sectional analysis of  $t = 12.5$  mm are considered to be identical to those obtained from testing of the  $t = 9.5$  mm test piece shown in Figure 10. Figure 13 shows the relationship diagram between the surface strain measured on the front of the gypsum board,  $\varepsilon_f$  (horizontal axis) to the strain measured on the back surface  $\varepsilon_b$  (vertical axis) of the gypsum board. The analysis result is represented by the symbol  $\bigcirc$  for  $t = 9.5$  mm and  $\Delta$  for  $t = 12.5$  mm. Results in red correspond to bending with the gypsum board oriented in the parallel direction, and those in blue correspond to the orthogonal direction. The experimental results are shown by solid and dotted lines (black:  $t = 9.5$  mm, gray:  $t = 12.5$  mm). Figures 12 and 13 show that the analysis results are in good agreement to the experimental results; thus, and the validity of the cross-sectional analysis of the gypsum board using a fiber model is confirmed. The first analysis data point, excluding the origin (zero) in Figure 12, is the elastic limit at which the gypsum first cracks.

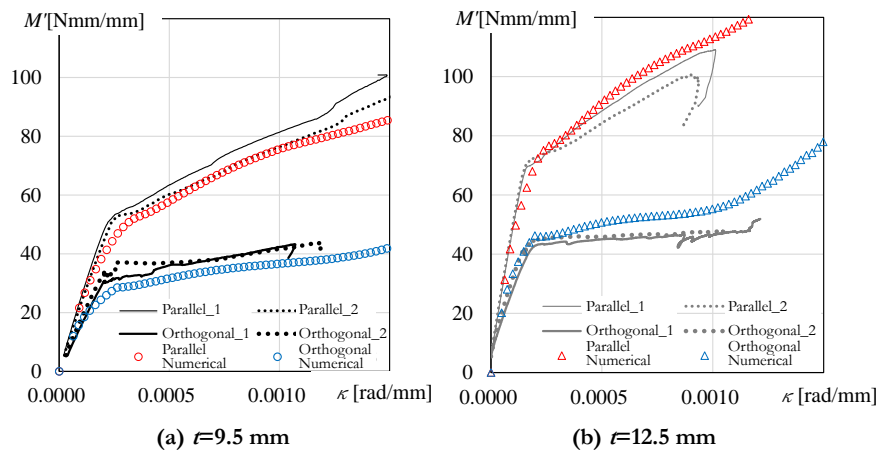


Figure 12. Comparison of of experimental and analytical results for the gypsum board moment-curvature relationship.

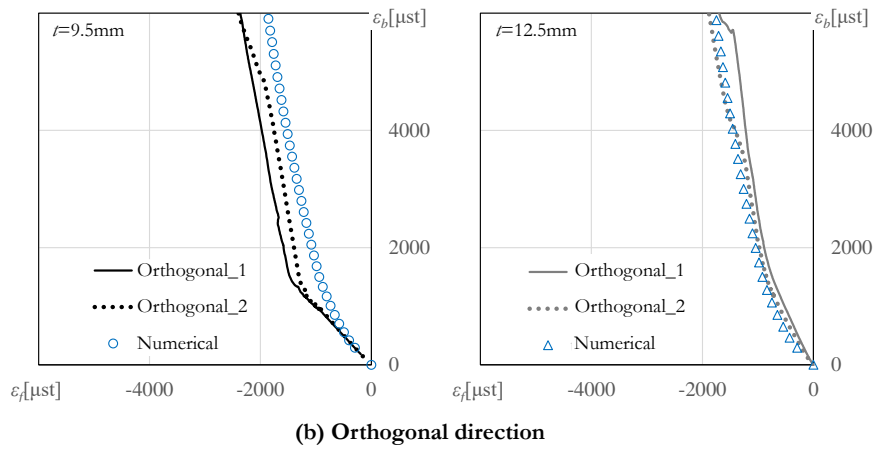
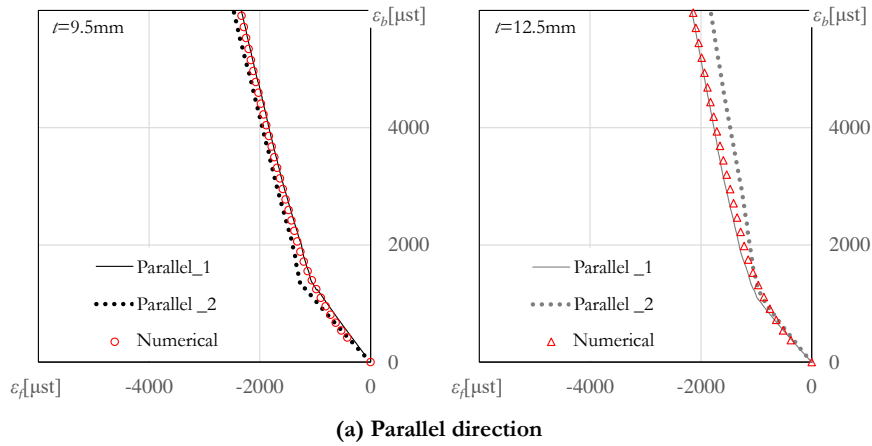


Figure 13. Comparison of experimental and analytical results for the front and back strain correlation

The distribution of stress through the gypsum board cross-section is shown in Figure 14 for the  $t = 9.5$  mm (fiber parallel direction) test piece. The distribution is shown at the elastic limit (Figure 14 (a)), the first break point (i.e., instance at which the flexural stiffness changes significantly; Figure 14 (b)), and the point at which gypsum crushing begins (Figure 14 (c)). From Figure 12 and 14, it is probable that the initial gypsum board crack propagates to half the board thickness. Furthermore, it is also possible that the gypsum board enters the non-linear region at a bending moment magnitude that is about half of the bending moment magnitude at the first break point; thus, the exact elastic region is relatively narrow.

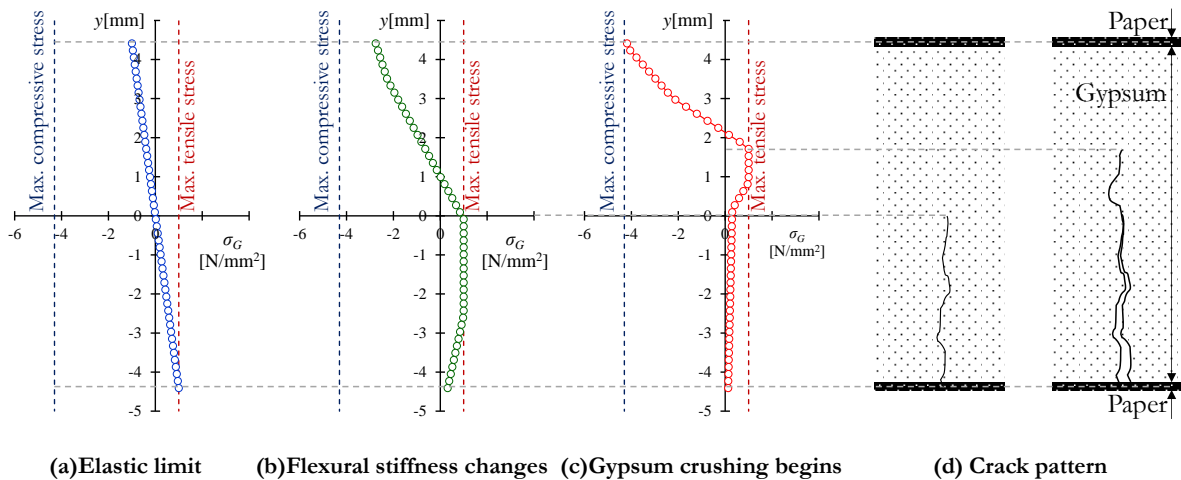


Figure 14. Distribution of stress of the gypsum board ( $t=9.5$  mm, Parallel direction)

## 4. CONCLUSION

In this paper, cross-sectional analysis of the gypsum board using the fiber model was carried out in order to investigate the mechanical properties of the gypsum board subjected to an out-of-plane bending moment. The analysis results were able to reproduce the experimental results well, and the fiber model was effective for cross-sectional analysis of the gypsum board. In the future, the behavior of the gypsum board when in-plane force and bending act on the gypsum board at the same time will be examined.

## ACKNOWLEDGEMENTS

This work was supported by JST Program on Open Innovation Platform with Enterprises, Research Institute and Academia and JSPS KAKENHI Grant Number JP16H02375.

## REFERENCES

- H. Yoshikawa, T. Tanabe. [1986] “An analytical study for the tension stiffness of reinforced concrete members on the basis of bond-slip mechanism,” *Journal of Japan Society of Civil Engineers*, Vol. 4, No. 366, pp. 93-102.
- Abdelhalim Benouis. [1995] “Comportement mecanique des ouvrages en plaques de platre sur ossature metallique,” *Phd thesis*, Sciences et Techniques du Bâtiment, École nationale des ponts et chaussées, France.
- T. Yokoyama, T. Odamura, K. Nakai. [2007] “Empirical response spectral attenuation relations for shallow crustal earthquakes,” *Journal of the Japanese Society for Experimental Mechanics*; Vol. 7, No. 2, pp. 129-135.
- JIS [2013] *Japanese Industrial Standards*, Japanese Industrial Standards Committee, Japan.
- Y. Sato, F. Sakuraba, S. Motoyui. [2020] “Structural Behavior of the Dry Partition Wall with Light-Gauge Steel,” *Proceedings of 17<sup>th</sup> World Conference on Earthquake Engineering*, Sendai, Japan.